Signals of fragment structures from a semiclassical transport equation in heavy-ion collisions

T.Reposeur, V.de la Mota and F.Sébille

Laboratoire Subatech, Université de Nantes/IN2P3/Ecole de Mines de Nantes F-44070 Nantes. France

C.O. Dorso

Departamento de Física, Facultad de Ciencias Exactas y Naturales, Universidad de Buenos Aires, Ciudad Universitaria-1428 Buenos Aires. Argentina

Abstract

Phase space bound structures generated from the semi-classical Landau-Vlasov (LV) description of the nuclear dynamics are analyzed. To this purpose a new satistical approach has been implemented for sampling configurations with fixed number of nucleons from the LV solution, on which the most bound density fluctuations in phase space are searched. The method is shown to reproduce correctly the global experimental trends on ^{36}Ar on ^{58}Ni at 32, 52 and 95 MeV/nucleon incident energies. This results open a new view of one body descriptions.

PACS: 25.70.-z, 21.60.Gx

1 Introduction

The disassembly of highly excited drops into a mixture of small aggregates and individual particles is nowadays one of the most interesting and challenging problems in non-equilibrium physics. In Nuclear Physics this phenomenon is present in the so-called multifragmentation in heavy ion collisions (HIC) at intermediate energies.

The multifragmentation process in HIC was predicted [1] to occur at high enough excitation by different approaches. From the experimental point of view, the multifragment emission has been evidenced by first generation 4π detectors [2] as an important decay channel. Recently, very efficient devices have been constructed [3] and a considerable amount of experimental results is currently available. Nevertheless, in spite of the existence of new and more refined data, the dynamical mechanisms leading to the disassembling of nuclear systems in several fragments are not yet fully understood.

Among the different theoretical approaches describing the dynamics of HIC at intermediate energies we will mention those based on some transport equation, like Vlasov- Uheling- Uhlenbeck (VUU) [4], Boltzmann- Uheling-Uhlenbeck (BUU) [5], the Landau- Vlasov (LV) [6] and the Boltzmann-Nordheim- Vlasov (BNV) [7] models. All these formalisms have in common the characteristic that they describe the reaction dynamics through the evolution of the one body distribution function in phase space. They have been successful in the description of global features of HIC reactions at intermediate energies as for example the collective flow, inclusive cross-sections, single particle spectra, etc. On the other hand the possibility of extracting information about fragment formation has been quite an elusive point. Most of the analysis performed so far have relied on simple cluster recognition algorithms which disregarded the role of momentum space [8]. On the other hand the role of fluctuations in phase space has shown to be of primarily importance in the formations of aggregates leading to fragments [9]. In this communication we explore the onset and evolution of bounded structures in phase space in the collision of ^{36}Ar on ^{58}Ni at 32, 52 and 95 MeV/nucleon recently performed at GANIL. In section II we briefly describe the LV formalism used to describe the collision dynamics. In order to extract information

of the fragment formation process a novel model is devised. Firstly, the one body distribution resulting from the LV formalism is described in terms of N-body configurations, taking special care that conservation laws are satisfied and that Pauli principle is not violated. Secondly, clusters are searched for on these configurations. This is described in section III. Results are finally shown in section IV and a discussion is presented.

2 The Landau Vlasov Model

The Landau-Vlasov model describes the dynamics of nuclear collisions through a semi-clasical transport equation for the one body distribution function in phase space $f(\vec{r},\vec{p})$. It consists in a free-flow or Vlasov term complemented by a Pauli-blocked Uehling-Uhlenbeck collision term $I_{coll}(f)$ [6],

$$\frac{\partial f}{\partial t} + \{f, H\} = I_{coll}(f) \tag{1}$$

where $\{\ ,\ \}$ stands for the Poisson bracket and H is the one-body Hamiltonian. This equation is solved by projecting $f(\vec{r},\vec{p})$ onto a moving basis of coherent states, which are frozen-width gaussians in coordinate and momentum spaces:

$$f(r,p) = \frac{A}{N}\sum_i \omega_i\ g_\chi(\vec{r} - \vec{r}_i)\ g_\phi(\vec{p} - \vec{p}_i) \tag{2}$$

The w_i are here the projection coefficients determined by the initial conditions, χ and ϕ the variances in coordinate and momentum space. A detailed description of the LV model can be found in Refs. [6, 15] and references quoted therein.

This model has been shown to reproduce accurately the equation of state of nuclear matter at zero and finite temperatures for many different interactions with zero or finite range [12]. Estimations of surface energy of semi-infinite nuclear matter are also correct [15]. It has been used to study dynamical instabilities arising from fluctuations in the spinodal zone for nuclear matter [14] and characteristic times were extracted for the spinodal decomposition. It has also been widely proven the success of this model

on the description of the nuclear dynamics in HIC at intermediate energies [11, 12, 13].

Concerning the Boltzmann-like collision term, we used in this work the isospin and energy dependent free nucleon-nucleon cross-section. We did not include any in-medium corrections, since in spite of intensive theoretical efforts [16, 17], they are not yet well known and they do not exceed 0.8 to 1 times the free value [16].

With respect to the one-body Hamiltonian in equation (1), we consider a simplified version of the zero-range Skyrme effective force, the so-called Zamick interaction [18]. With this force the one-body potential reads:

$$V_q(\rho, \xi) \; = \; t_0 \; \rho \; + \; t_3 \; \rho^{\nu+1} \tag{3}$$

where ρ is the local density: and t_0, t_3 and ν are parameters adjusted to give saturation properties of infinite symmetric nuclear matter. In particular, the saturation density value is ρ_∞=0.145 fm^{-3}. In our case: $t_0 \; = \; -356 MeV/\rho_\infty$; $t_3 \; = \; 303 MeV/{\rho_\infty}^{\frac{7}{6}}$, $\nu \; = \; \frac{1}{6}$. We use this very simple force in order to give a first illustration of global dynamical trends which, at the same time, can serve as a test of the method that we describe below. Nevertheless, further investigations using more realistic forces, which take into account for instance surface terms, should be performed. This kind of calculations are now in progress.

3 Cluster Analysis

The Landau-Vlasov equation gives the time evolution of the one-body density of a system of A interacting particles. It is obtained from the projection of the Liouville equation corresponding to the total A-body distribution function onto the one-body phase space Γ, after truncation of a hierarchy of correlation patterns. This procedure gives rise to an extended mean-field description which takes dissipative processes into account. These processes are given in terms of a Boltzmann-like collision kernel.

A one-body distribution function represents at each time the mean occupation in an element of volume $d^6\Gamma = d^3r \; d^3p$ in Γ space. This represents the

mean number of particles in $d^6\Gamma$ when a number M of experiments (each one involving A particles) have been performed. Let us call $C_i(\vec{r},\vec{p})$ the particle configuration whose coordinates lie within $d^6\Gamma$ around $(\vec{r},\vec{p})$ for each individual experiment, and define Θ_Γ an operator giving the number of particles in C_i. Then the LV distribution function can be viewed as an microcanonical ensemble average of microscopic "A-body" configurations $C_i(\vec{r},\vec{p})$, such that:

$$d^6N = f(\vec{r},\vec{p})\; d^3r d^3p = \frac{1}{M}\sum_{i=1}^{M}\Theta_\Gamma(C_i(\vec{r},\vec{p}))\; d^6\Gamma \tag{4}$$

where d^6N gives the number of particles in $d^6\Gamma$. Conversely [10] , M' configurations of A particles can be generated by choosing phase space coordinates according to the LV distribution function. Such a mapping must respect the following conditions: i) conservation of a given set of relevant observables with respect to the mean behaviour, and ii) Pauli exclusion principle. Consider the most general ensemble of A-body states, satisfying Eq.(4) together with conditions i) and ii). It contains informations about the dissipative behaviour of the system generated by a mean-field-plus-collisions description, given by the LV model, since it is constructed from a truncated hierarchy of correlations. Not only the individual C_i are elements of this ensemble, but also many more configurations which are consistent with the solutions of the exact many-body problem.

In this spirit the procedure we adopted is the following: a) at each time t, from the complete set, A=94 gaussians were picked at random one by one. In this way, we get a sampling according to the one-body density resulting from the L-V model. It is also important to note that this is a minimum bias mapping. b) at each step, i.e. each time a new gaussian is taken, we checked that

$$\frac{\delta x_{ij}^2}{x_0^2} + \frac{\delta p_{ij}^2}{p_0^2} \geq 1 \tag{5}$$

with $\delta x_{ij}^2 = [\overrightarrow{x_i} - \overrightarrow{x_j}]^2$ and $\delta p_{ij}^2 = [\overrightarrow{p_i} - \overrightarrow{p_j}]^2$, x_0 and p_0 are normalization constants satisfying the relation $(x_0 p_0)/\hbar = 1$, thus insuring that Pauli exclusion principle is not violated. In this case we have considered a lattice structure assuming a body-centered cubic net with close packing. x_0 is then calculated as the distance to the nearest neighbour in the net. c) once the complete set is thus generated, we check for the conservation (with respect

to the LV description) of total potential energy, total kinetic energy, momentum and angular momentum. d) if condition c) is satisfied the configuration is accepted, otherwise it is rejected. In order to obtain reliable information on observables typically measured in experiments, this process is performed for a wide range of impact parameters b, as many times as configurations are required for the calculation of the fragment spectra (according to the geometrical law $dn = 2\pi b\ db$).

It is important to point out that in order to calculate the magnitudes involved in condition c) a prescription must be given to calculate the energy of the configurations resulting from the mapping. In order to keep the consistency with the L-V formalism used to generate the primordial one body distribution function we adopt the following recipe: we assign to each point of the projected configuration a Gaussian with a width that is a function of the number of points of the projected configurations (A in this case). This new set of Gaussians interact with the same potential as described in Eq. (3). Taking a set of initial configurations as reference we fix the width of the gaussians in order to conserve volumes in phase space. For a uniform distribution of gaussians, this gives the condition $\sigma' = (N/A)^{1/6}\ \sigma$, where σ' and σ stand for the square roots of the new variances α (or β) appearing in the sampling, and of those in the original LV distribution function χ (or ϕ), respectively. Once this is accomplished the width is fixed for the rest of the calculation. In this work we used $N/A = 60$.

When this configurations are built the fragment recognition procedure is as follows: According to [9] a cluster ζ is defined as that set of particles, denoted by the sub indices i , which satisfies the following condition

$$\forall i \in \zeta, \qquad e_i = T_{iCM} + \sum_j V_{ij} < 0 \tag{6}$$

where T_{iCM} is the kinetic energy of particle i calculated in the C.M. of the cluster ζ. Here V_{ij} denotes the interaction energy between particles i and j, both belonging to the same cluster ζ ; i.e. all particles must be bound.For a system of particles we define the cluster decomposition as a partition of the total system into subsets, such that, for each subset condition (6) is satisfied, i.e. each subset is a cluster. Because this condition can be satisfied by more that one partition we introduce the following additional condition: *a cluster structure is a decomposition of the system in which the total binding energy is maximum when each cluster is considered as non interacting with the others.*

As it can be easily seen this is a very complicated task, because the binding energy is calculated in the center of momentum of each subset of the partition, as a consequence, the problem is highly self consistent. To solve it, an algorithm in the spirit of simulated annealing was developed (ECRA) [9]. It is clear that this cluster definition is free from arbitrary "clusterization parameters", on the other side this method is statistical in nature and although we can be confident that we will be quite close to the maximizing partition, we cannot be sure that the true maximum has been reached. It should be emphasized at this point that, being it possible to apply this method at any point in the evolution of the system, there will be a stage in which what we are recognizing as clusters is the set of most bound density fluctuations in phase space. During this stage particles are close together in q space and no cluster structure can be recognized by standard configuration (MST) cluster recognition algorithms. At later, asymptotic, times the colliding system will evolve into a dilute mixture of free nucleons and small aggregates, in which clusters will be well separated in space and then we can call them fragments.

The one-body density ρ resulting from the projection onto the r-space of the LV distribution function is show in Fig 1, in full lines, for Ar + Ni at 95 MeV/nucleon and b=0.5 fm, at different times. In this figure, the coordinate r is paralell to the beam axis, in the center of mass frame. Together with this quantity we show, in dashed lines, the densities as calculated from the superposition of 20 A-particles mappings. As it can be readily seen the agreement is very good even at asymptotic times, where the densities strongly fluctuate. These results show the consistency of our procedure at the sampling level.

4 Comparison with experimental results

In this section we show the results of our calculation in the case of the ^{36}Ar + ^{58}Ni reaction at 32, 52 and 95 MeV/nucleon, recently studied at GANIL using the 4π detector INDRA [20],[21],[22].

The bare results of the above described method were further processed in the following way: i) we have removed what we call "unrealistic clusters" as for instance diprotons; ii) a simplified version of an experimental filter has been applied in order to simulate the detector acceptances (angular and energy detection thresholds).

In Fig. 2 we show the evolution of the charged product multiplicity for complete events with the incident energy. In the left panel the experimental results of ref [20] are shown for incident energies of 32,52 and 95 MeV/nucleon, on the right panel we show the results of this calculation. From the comparison between left and right panels we observe that, in spite of the low statistics in the calculation, the main characteristics of the bell-shaped distributions are reproduced. We see that in both cases the curves broaden and the maxima are shifted towards higher multiplicity values when the incident energy increases. In particular, at 95 MeV/nucleon this last quantity attains values which are close to the total charge of the system. Nevertheless, in this case, the theoretical histogram is too wide with an important contribution in the high multiplicities region. This result is not very surprising since, on one side, the LV distribution function does not contain dynamical multiparticle correlations and, on the other side, in the clusterization procedure the implemented effective interaction is the same as in the LV dynamics (Eq.3). Even if this kind of force describes rather well the mean field properties, it does not account for the quantum effects required to generate bound fragments of few nucleons. A consequence of this is the fact that the charged particle multiplicity is overestimated. This effect is naturally more marked at the highest energy.

Also in complete events, the intermediate mass fragments (IMF) multiplicities normalized to their areas [20] are shown in Figs.3 a)-b) at different incident energies. Here, IMF stands for those fragments with charge bigger or equal to 3. Accordingly to the experimental yields, the theoretical IMF distribution (Fig. 3.b) is dominated by 2 and 3 IMF independently of the energy. The maximum IMF multiplicity is nevertheless lower in our calculations than in the experiment, except for the case at 95 MeV/nucleon incident energy, in which the general shape of the histograms are very similar. In fact, at 32 and 52 MeV/nucleon the tails of the distributions corresponding to low probability events do not agree with the data. In our calculations, the number of IMF is clearly lower and the onset of "vaporization" [21], which corresponds to those rare events in which zero IMF are detected, is not found at incident energies below 95 MeV/nucleon. According with the discussion of the previous figure the absence of these events, mainly at low energy, are not only related to our low statistics but also to the incomplete one-body description of the collisional process with a simple local force.

In Figs. 4 we show the mean number of IMF as a function of charged

product multiplicities. In this case experimental results [22] (stars) for only two energy values are available (32 and 95 MeV/nucleon in Figs. 4 (a) and (b), respectively). From the comparison it is seen that the general shapes are qualitatively reproduced by our results (full dots). On one side, both curves attain a maximum value which is nearly the same for both energies. On the other side, the range of charged product multiplicities is shifted towards higher values at 95 Mev/nucleon. As expected, due to the same reasons as in the preceding figures, the maximum value of the mean number of IMF is underestimated in roughly 1 IMF. This results from the fact that the interaction used in the algorithm which determines the most bound structures lacks of quantum and surface effects. The consequences of this in Fig. 4(b) is to stretch the results along the absissa and to compress them along the ordinate axis with respect to the data. Despite these effects, our results exhibit the experimetally observed saturation of the maximum mean number of IMF with the incident energy, which is characteristic of the phase space geometry generated in the initial violent stage of the reaction.

5 Conclusions

In this communication we presented a novel method for fragmentation analysis in one-body (Landau Vlasov) description of nuclear collisions. Its main idea is to build A-body configurations coherent with the kinetic one-body distribution. This mapping is performed in such a way that the initial one-body distribution is well reproduced by the superposition of the projected configurations. No extra correlations are introduced. The only restriction is that no violation of Pauli principle is allowed. Moreover, conservation of total energy (potential and kinetic), total momentum and total angular momentum, with respect the LV description, is carefully enforced. Finally a cluster recognition algorithm in the spirit of the ECRA is applied. This method is free from arbitrary clusterization parameters and can be applied at any stage of the evolution, even at very early dense ones, thus allowing for the analysis of the time evolution of the most bound density fluctuations in phase space.

The input of the above mentioned method was the one-body distribution resulting from a LV simulation, using a very simple force, i.e. the Zamick one. The comparison between the experimental results and our calculations

are quite encouraging. It is seen that in all the cases investigated we can reproduce the general trends. Since no quantum effects and no additional correlations than those present in the kinetic LV description are injected, this method cannot exactly describe fragment spectra, in particular small clusters are not reliable. The interesting consequence of this work is that a one body description as the LV model plus a suitable fragment recognition method is able to correctly reproduce the global trends of the experimentally measured observables which are relevant for fragmentation even when fluctuations are analyzed (i.e. Fig 2). These results open new questions about the origin of this predictive power on semi-classical one-body theories and new works on this subject are now in progress.

Aknowledgements: One of us C.O.D. gratefully aknowledges partial finantial support from UBA grant EX-070. V.d.l.M. is grateful to FCEN-UBA for partial finantial support and kind hospitality. This work has been partially founded by CNRS-CONICET agreement of collaboration number Z17062.

References

[1] Moretto, L.G. and Wozniak, G.J.: Ann. Rev. of Nucl. and Part. Sci.: Jackson, J.D. Ed. **43** 379 (1993)

[2] Bizard, G. et al.: Nucl. Instr. Meth. **A224** 483 (1986); Bougault, R. et al.: Nucl. Instr. Meth. **A259** 473 (1987); Peghaire, A. et al.: Nucl. Instr. Meth. **A295** 365 (1990); Rudolf, G. et al.: Nucl. Instr. Meth. **A307** 325 (1991)

[3] Chbihi, A. et al.: First European Biennal Workshop on Nuclear Physics, Megeve, France, 1991

[4] Kruse, H., Jacak, B.V., Stocker, H.: Phys. Rev. Lett. **B54** 289 (1985)

Kruse, H., Jacak, B.V., Molitoris, J., Westfall, G. and Stocker, H.: Phys. Rev. **C31** 1770 (1985)

[5] Bertsch, G. and Das Gupta, S.: Phys. Rep. **160** 189 (1989)

[6] Gregoire, C., Remaud, B., Sebille, F., Vinet, L. and Raffray, Y.: Nucl. Phys. **A585** 317 (1987); Schuck, P., Hasse, R.W., Jaenicke, J., Grégoire, C., Remaud, B., Sébille, F. and Suraud, E.: Prog. in Part. and Nucl. Phys. **22** 181 (1989)

[7] Bonasera, A., Gulminelli, F. and Molitoris, J.: Phys. Rep **243** 1 (1995)

[8] Aichelin, J.: Phys. Rep. **202** 233 (1991)

[9] Dorso, C.O. and Randrup, J.: Phys. Lett. **B301** 328 (1993); Dorso, C.O. and Balonga, P.: Phys. Rev. **C50** 991 (1994); Dorso, C.O. and Aichelin, J.: Phys. Lett. **B345** 197 (1995); Aranda, A.,Dorso, C.O., Furci, V. and Lopez, J.: Phys. Rev. **C52** 3217 (1995); Dorso, C.O. and Strachan, A. : Phys. Rev. **B** in press

[10] Dorso, C. and Donangelo, R.: Phys. Lett. **B244** 165 (1990); Donangelo, R., Dorso, C.O. and Marta, D.: Phys. Lett. **B263** 14 (1991)

[11] Remaud, B., Grégoire, C., Sébille, F. and Schuck, P.: Nucl. Phys. **A488** 423c (1988)

[12] Sébille, F., Royer, G., Grégoire, C., Remaud, B. and Schuck, P.: Nucl. Phys. **A501** 137 (1989)

[13] de la Mota, V., Sébille, F., Farine, M., Remaud, B. and Schuck, P.: Phys. Rev. **C46** 677 (1992)

[14] Idier, D., Benhassine, B., Farine, M., Remaud, B. and Sébille, F.: Phys. Rev. **C48** 48 (1993)

[15] Idier, D., Farine, M., Remaud, B. and Sébille, F.: Ann. Phys. **Fr. 19** 159 (1994)

[16] Cugnon, J., Lejeune, A. and Grangé, P.: Phys. Rev. **C35** 861 (1987)

[17] Faessler, A.: Nucl. Phys. **A495c** 103 (1989)

[18] Zamick, L.: Phys. Lett. **B45** 313 (1973)

[19] Wong, C. and Davies, K.: Phys. Rev. **C28** 240 (1983)

[20] De Filippo, E. et al.: Proc. XXXIII Winter Meeting on Nuclear Physics, Bormio (Italy), Ed. I. Iori, Univ. of Milano, 1995

[21] Bacri, Ch.O. et al.: Phys Lett. **B353** 27 (1995)

[22] Steckmeyer, J.C. et al.: Proc. XXXII Winter Meeting on Nuclear Physics, Bormio (Italy), Ed. I. Iori, Univ. of Milano, 1994

Figure Captions

Fig.1) In this Figure we show the projected one body density resulting from the L-V formalism together with the same quantity as calculated from the superposition of 20 N-particles mapping.

Fig.2) Evolution of the charged product multiplicity for complete events as a function of the incident energy. On the left we show the experimental results [20], on the right panel the calculated values.

Fig.3) Intermediate mass fragments (IMF) multiplicities normalized to their areas for complete events [20] at different incident energies: 32 (full line), 52 (dashed line) and 95 (dotted line) MeV/nucleon. The experimental values [20] are plotted in (a) and the results of the present calculation in (b).

Fig.4) Mean number of IMF as a function of charged product multiplicities for 32 (a) and 95 MeV/nucleon (b). The experimental data [22] are represented with stars and our theoretical results with full dots.

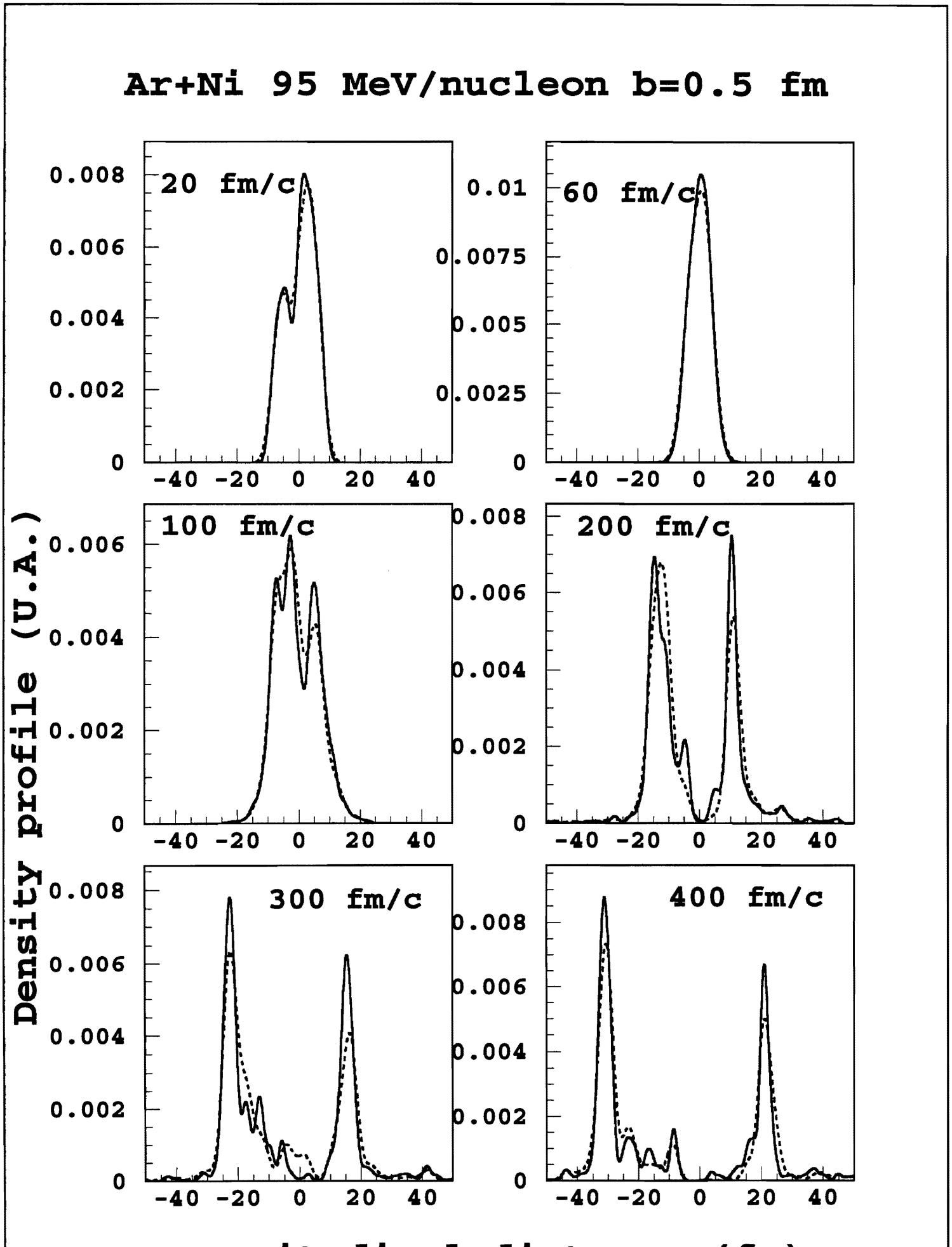
Ar+Ni 95 MeV/nucleon b=0.5 fm
20 fm/c
60 fm/c
100 fm/c
200 fm/c
300 fm/c
400 fm/c
Density profile (U.A.)
Longitudinal distance (fm) .

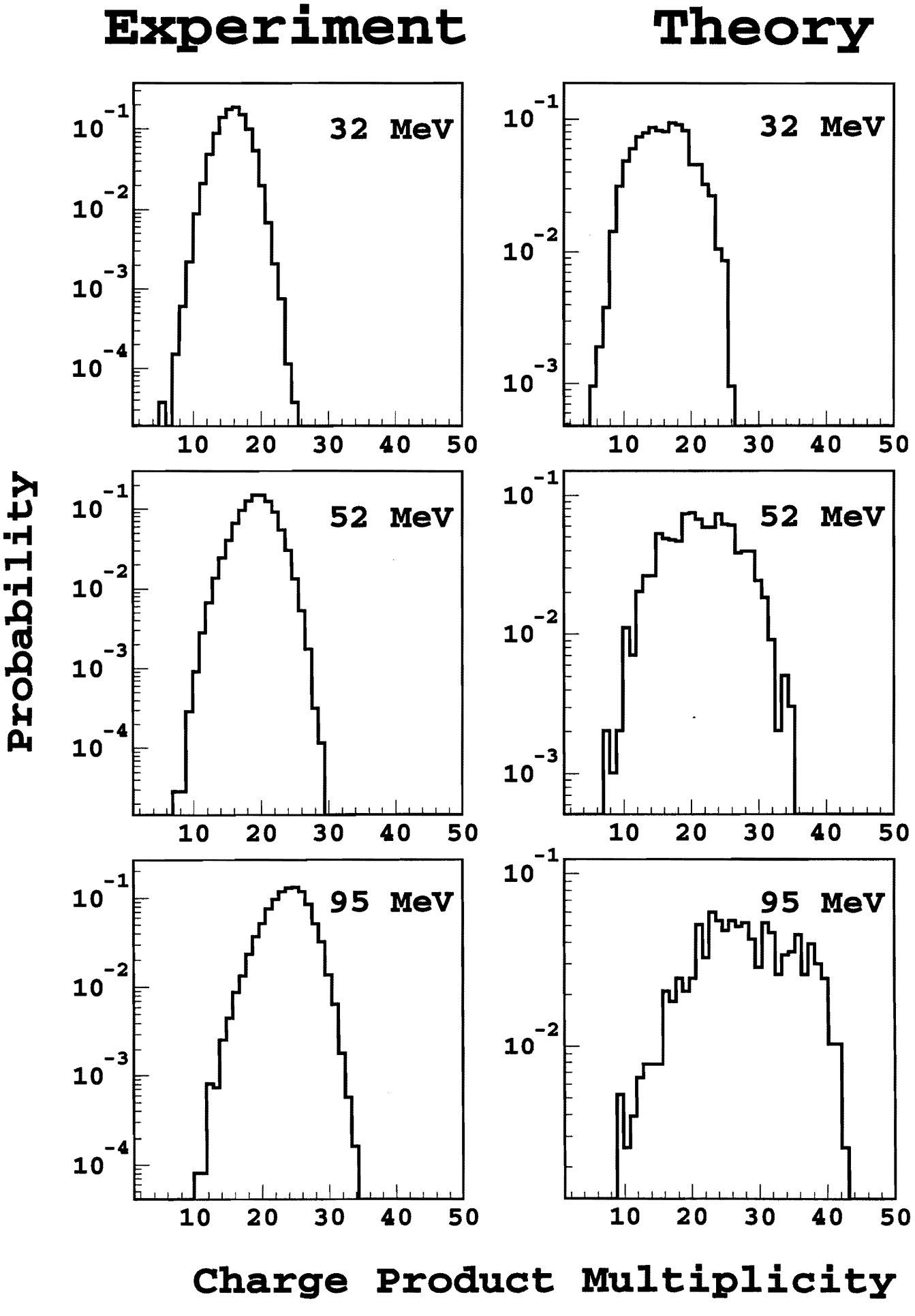
Experiment
Theory
32 MeV
52 MeV
95 MeV
Probability
Charge Product Multiplicity

FIGURE 2

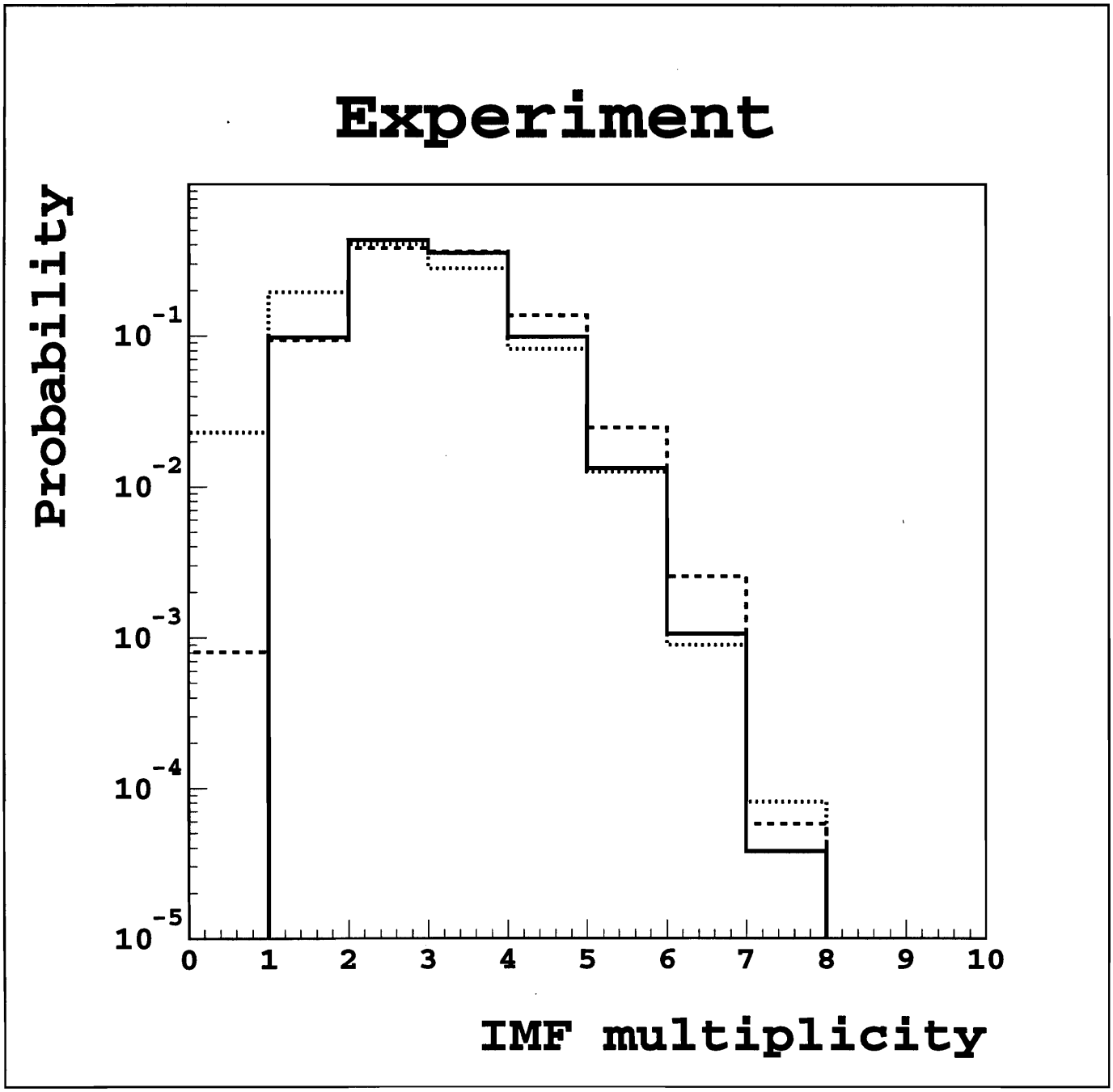
Experiment
Probability
10^{-1}
10^{-2}
10^{-3}
10^{-4}
10^{-5}
0
1
2
3
4
5
6
7
8
9
10
IMF multiplicity

FIGURE 3-a

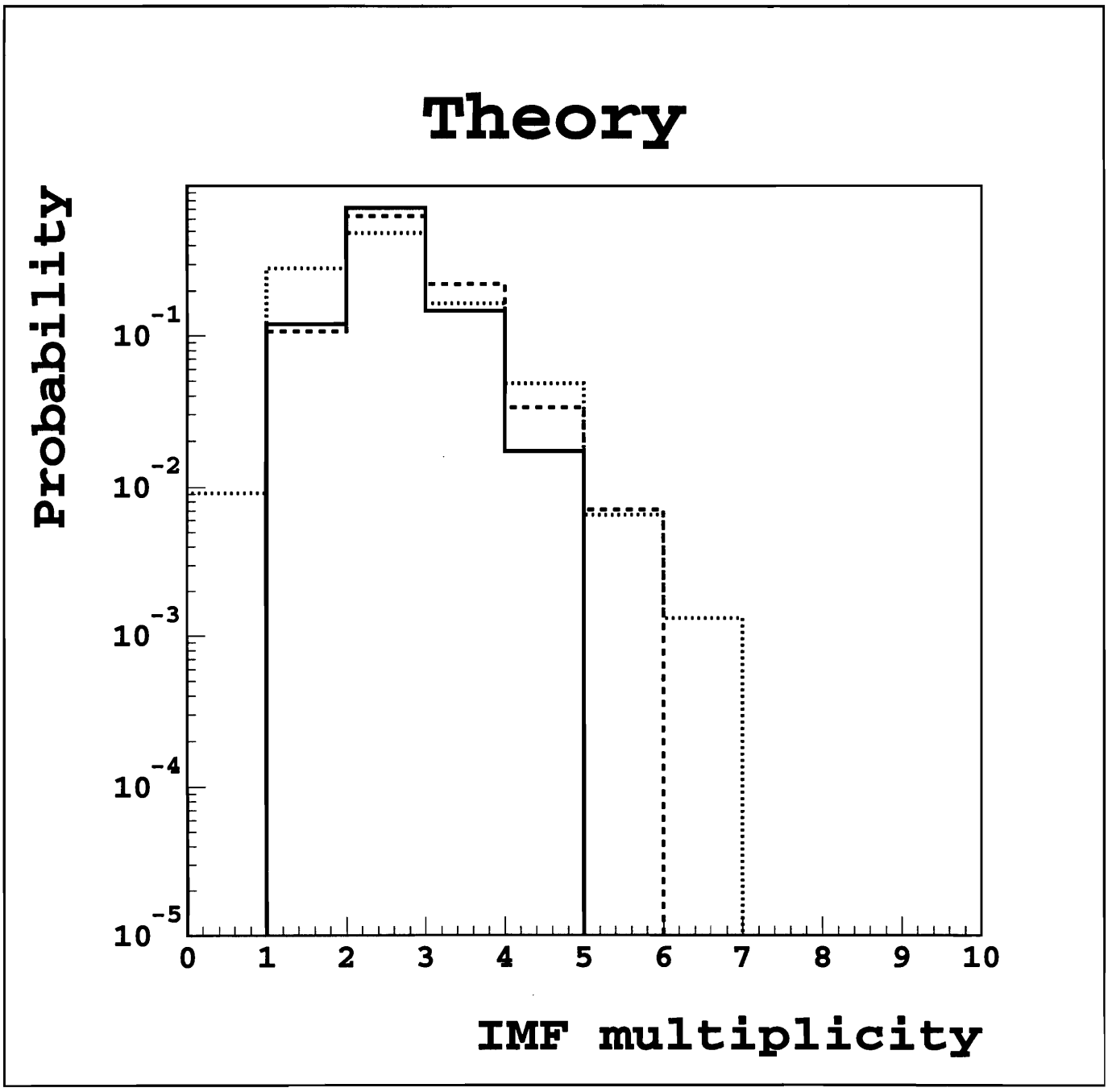
Theory
Probability
10^{-1}
10^{-2}
10^{-3}
10^{-4}
10^{-5}
0
1
2
3
4
5
6
7
8
9
10
IMF multiplicity

FIGURE 3-b

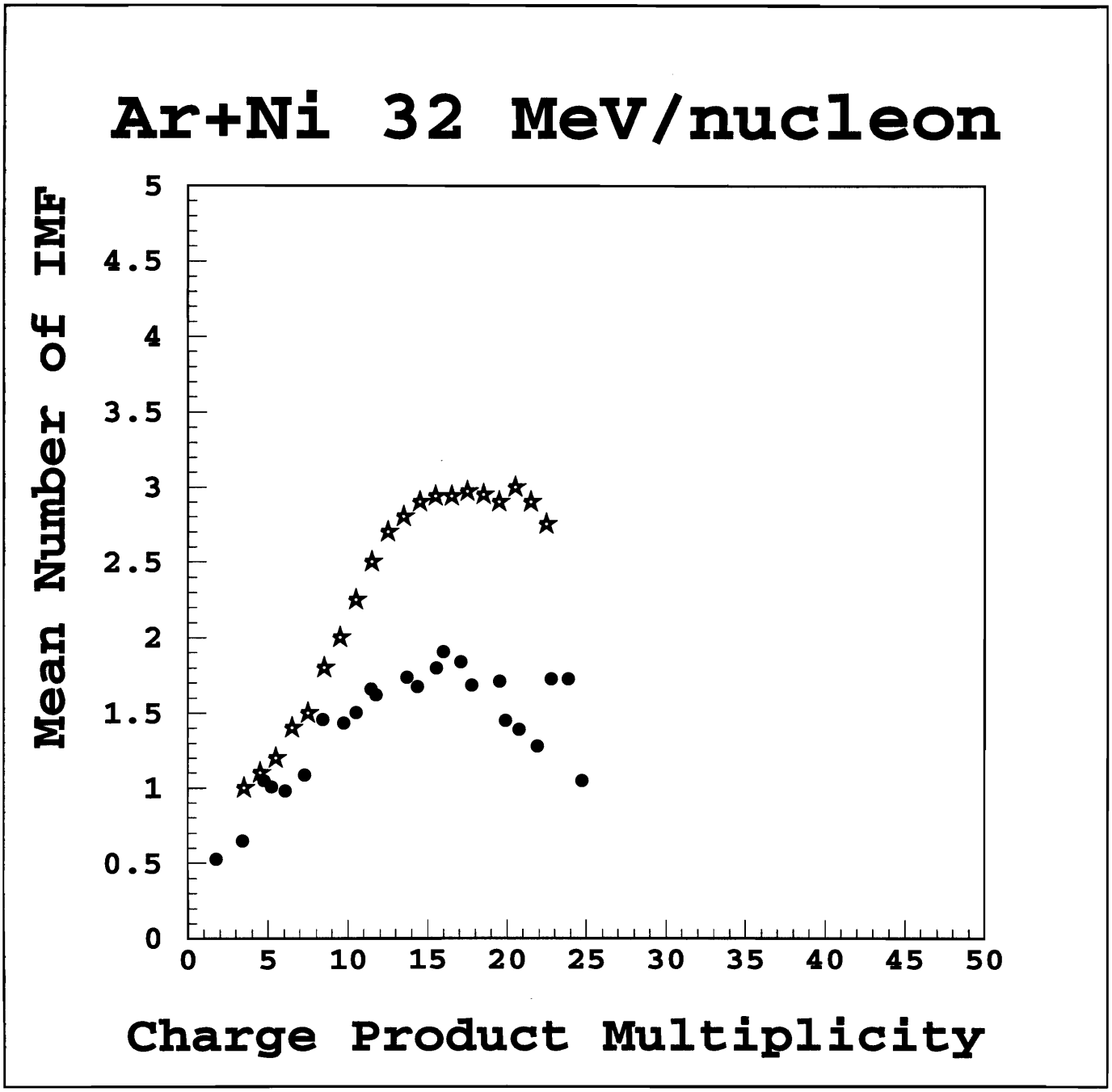
Ar+Ni 32 MeV/nucleon
Mean Number of IMF
0
0.5
1
1.5
2
2.5
3
3.5
4
4.5
5
0
5
10
15
20
25
30
35
40
45
50
Charge Product Multiplicity

FIGURE 4-a

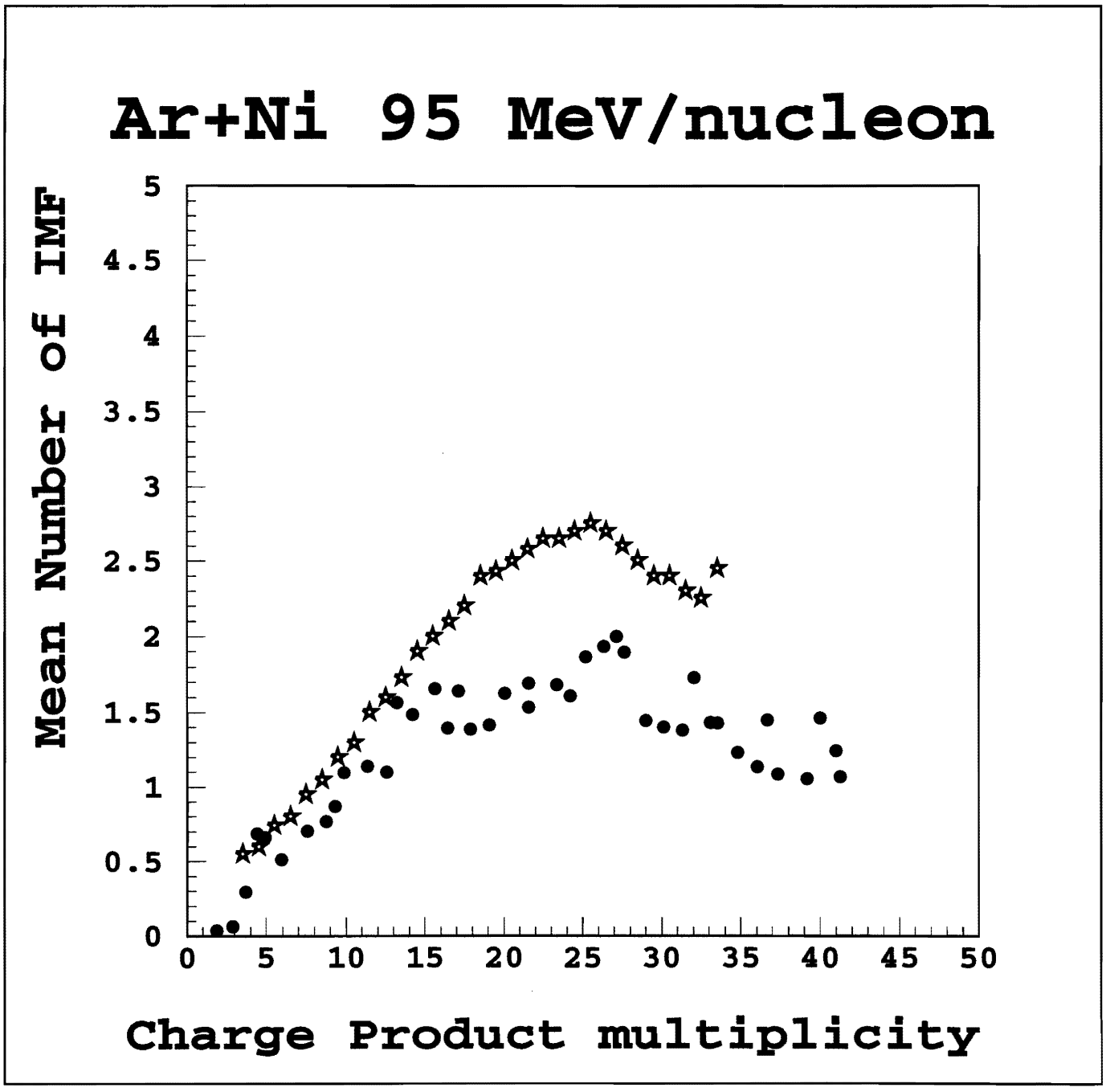
Ar+Ni 95 MeV/nucleon
Mean Number of IMF
0
0.5
1
1.5
2
2.5
3
3.5
4
4.5
5
0
5
10
15
20
25
30
35
40
45
50
Charge Product multiplicity

FIGURE 4-b